J. Chem. Eng. Data 1986, 31, 309–312

Thermodynamics of Concentrated Electrolyte Mixtures. 8. Apparent Molal Volumes, Adiabatic Compressibilities, and Hydration Numbers of Aqueous $ZnBr_2$, $CaBr_2$, and NaBr at 25 °C

Waclaw Grzybkowski[†] **and Gordon Atkinson***

Department of Chemistry, University of Oklahoma, Norman, Oklahoma 73019

Densities and sound velocities of aqueous solutions of $ZnBr_2$, $CaBr_2$, and NaBr have been measured in the ionic strength range 0–8.0 at 25 °C. The results are used to calculate the apparent molal volumes, adiabatic compressibilities, and total hydration numbers. The properties of the solutions are discussed and the very peculiar properties of the $ZnBr_2$ solutions have been interpreted in terms of complex formation and the influence of the solutes on the hydration structure. The Pitzer formalism is used to describe the properties of the $CaBr_2$ and NaBr solutions.

Introduction

Recently new attention has turned to the properties of concentrated solutions of electrolytes. The Pitzer ion-interaction model and the accompanying formalism have been successfully used to describe the thermodynamic properties of strong electrolytes (*1*). In previous papers we reported the corresponding treatment of the *PVT* properties of $CaCl_2$ and NaCl solutions as well as their mixtures (*2*, *3*). The apparent molal volumes, adiabatic compressibilities, and expansibilities were obtained and analyzed in terms of the Pitzer equation. The results obtained for the mixtures were compared with predictions based on the specific interaction theory.

In the present paper we report the data obtained for $ZnBr_2$, $CaBr_2$, and NaBr at 25 °C. There is a growing interest in using such solutions in various industrial processes. One example of this is the application as "completion fluids" in petroleum and gas well drilling. Therefore, accurate knowledge of the *PVT* properties of the systems is highly desirable. Moreover, there is a need to test the range of applicability of the Pitzer formalism for systems such as $ZnBr_2$ solutions where very strong interactions occur and stable complexes exist.

Numerous studies on the structure and thermodynamic properties of $ZnCl_2$ solutions have been performed. However, relatively few data have been obtained for $ZnBr_2$ solutions and their structure is not clear. In recent work Kalman (*4*) studied electron and X-ray scattering as well as Raman spectra and reestablished that the dominant species in aqueous solutions of $ZnBr_2$ are the octahedral $Zn(H_2O)_6^{2+}$ and the tetrahedral $ZnBr_2(H_2O)_2$, $ZnBr_3(H_2O)^-$, and $ZnBr_4^{2-}$ complexes. The same conclusion was drawn by Tamura (*5*) from ultrasonic absorption studies, indicating that some configurational changes occur accompanying complex formation. Complex formation is responsible for the abnormal physical properties of $ZnBr_2$ and $ZnCl_2$ aqueous solutions. It is reflected in the variation of the activity coefficients with concentration, distinguishing the zinc halides from other electrolytes. This peculiar behavior was mentioned earlier by Robinson (*6*). The effect is especially distinct if the activity coefficients of $ZnBr_2$ are shown together with the corresponding data for $CaBr_2$ solutions. In Figure 1 the data evaluated by Goldberg (*7*, *8*) are plotted as log $\gamma_\pm$ against the square root of ionic strength. As is seen, the activity coefficients of $ZnBr_2$ behave like those of $CaBr_2$ only for very dilute solutions. The differences occurring at higher concentration are rather striking. The most characteristic feature of these differences is the existence of inflection points at 0.65 and 1.5 M. Therefore, it is not surprising that the activity coefficients of $ZnBr_2$ could not be fitted satisfactorily to the appropriate Pitzer equation. Moreover, the activity coefficients of $ZnBr_2$ vary within relatively narrow limits, from 0.5064 for $m = 0.3$ to 0.6741 for $m = 4.0$ M, while the activity coefficients of $CaBr_2$ change from 0.4909 up to 6.482 in the same concentration range.

The volume properties of $ZnBr_2$ in water were also studied. Nicholas and Reich (*9*) analyzed the variation of the partial molar volumes of water and $ZnBr_2$ as well as the viscosity and conductivity. The observed effects were discussed in terms of the changes in the structure of water. It should be noted, however, that they did not consider the contribution due to complex formation.

Experimental Section

All reagents were obtained from Fisher Scientific Co. and were Certified ACS grade. Calcium bromide was prepared from the carbonate by dissolving in hydrobromic acid, followed by crystallization. Zinc bromide and sodium bromide were also purified by repeated crystallization. The traces of bromine were removed by the use of activated charcoal. The stock solution of $ZnBr_2$ was tested for hydrolysis. Dilution up to 0.005 M did not result in the precipitation of the corresponding hydroxy salts.

The stock solutions of $ZnBr_2$ and $CaBr_2$ were analyzed for the metals by standard EDTA titrations (*10*) in addition to the gravimetric determination of bromides in the form of AgBr (*10*). The stock solution of NaBr was analyzed by drying to constant weight. The results obtained by the two different methods agree to within ±0.07%.

The stock solution as well as solutions for measurements were prepared by using 18.4 MΩ·cm deionized water. Solutions for measurements were prepared by weighed dilutions of the corresponding stock solutions.

The densities were measured with a Sodev vibrating tube densimeter and the sound velocities with a Nusonics "sing-around" velocimeter. The instruments were calibrated with NaCl solutions by using the Millero (*12*) and Desnoyers (*13*) data. The measurements were carried out at 25 °C and the temperature was controlled to ±0.005 °C with a Tronac CT bath. Details of the procedures were identical with those described previously (*2*, *3*). The values of density and sound velocity in pure water used during calibration and in the following calculation were 0.997 047 $g\cdot cm^{-3}$ and 1496.69 $m\cdot s^{-1}$, respectively.

Results and Discussion

The relative densities and sound velocities of the $ZnBr_2$, $CaBr_2$, and NaBr solutions are given in Table I while Figure 2

[†] Technical University of Gdansk, 80-952 Gdansk, Poland.

0021-9568/86/1731-0309$01.50/0 © 1986 American Chemical Society

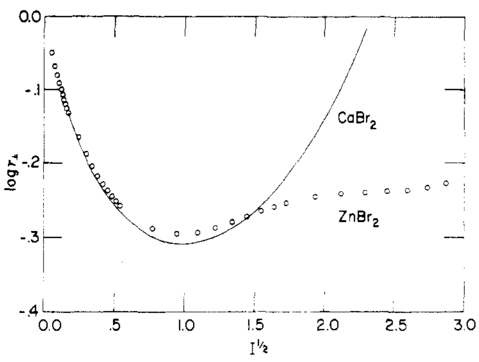

Figure 1. Plot of the logarithm of the activity coefficient against the square root of ionic strength at 25 °C.

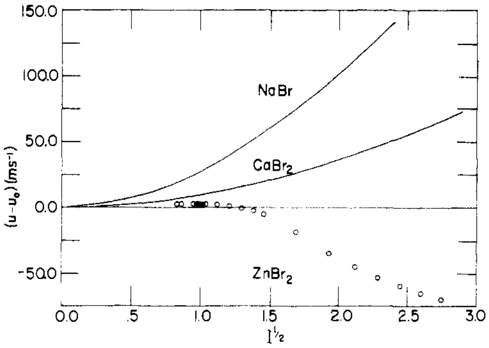

Figure 2. Plot of the relative sound velocity against the square root of ionic strength at 25 °C.

shows the relative sound velocities plotted against the square root of the ionic strength.

The results obtained for NaBr agree very well with the low concentration data reported by Millero (*14*) and can be fitted to the common equation

$$u - u_0 = 0.3944m^{1/2} + 25.6753m + 1.2834m^{3/2} - 0.8007m^2 \tag{1}$$

where u and u_0 are sound velocities in the solutions and water, respectively, and the RMSD value for both sets of data is 0.05 $m{\cdot}s^{-1}$. The data for the $CaBr_2$ solutions are described satisfactorily by using a similar equation

$$u - u_0 = 1.1261m^{1/2} + 18.6214m + 11.8129m^{3/2} - 4.7430m^2 \tag{2}$$

with RMSD = 0.06 $m{\cdot}s^{-1}$.

The most striking feature of the data presented in Figure 2 is the very peculiar shape of the curve obtained for the $ZnBr_2$ solutions. The relative sound velocities in dilute solutions are positive but very small, but become negative and large in magnitude when the concentration of the solute is increased. Thus, it is not surprising that the relative sound velocities for the $ZnBr_2$ solutions cannot be described by an equation of the form used above. Negative values of relative sound velocities are not common. They have been observed in only a few systems, and in all cases only for salts displaying rather strong structure-breaking properties such as NaI, KI, and CsCl solutions (*14*). Further, it should be noted that the sharp downturn of ($u - u_0$) for $ZnBr_2$ occurs at close to the same concentration as the second inflection point in the activity coefficient curve.

The sound velocity and density data for the solutions can be used to calculate the adiabatic compressibility through Newton's equation

$$\beta_s = \frac{1}{d}\left(\frac{\partial d}{\partial P}\right)_s = \frac{1}{u^2 d} \tag{3}$$

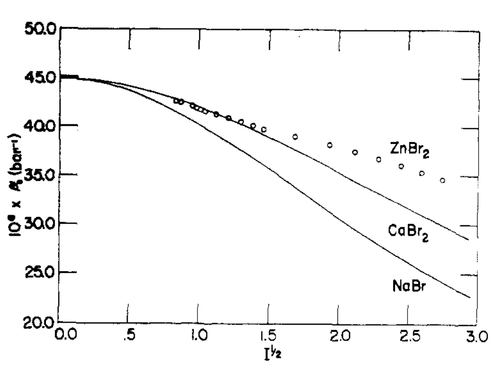

Figure 3. Plot of the adiabatic compressibility against the square root of ionic strength at 25 °C.

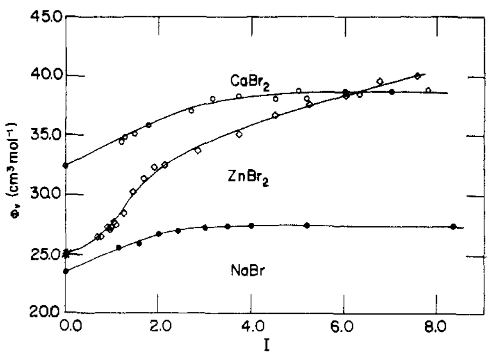

Figure 4. Plot of the apparent molal compressibility against the ionic strength at 25 °C. The limiting parameters are indicated as asterixes.

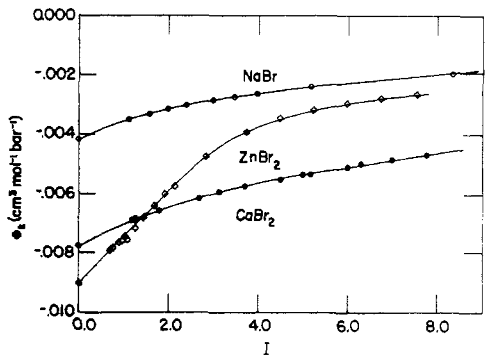

Figure 5. Plot of the apparent molal volume against the ionic strength at 25 °C. The limiting parameters calculated from literature data are indicated as asterixes.

In Figure 3 the compressibilities are plotted vs. $I^{1/2}$ for the three salts. The $ZnBr_2$ becomes substantially more compressible than the "typical" 2–1 salt, $CaBr_2$, at a relative low concentration.

The apparent molal volumes, ϕ_V, and adiabatic molal compressibilities, $\phi_{K(S)}$, were calculated by using the equations

$$\phi_V = \frac{M_2}{d} - \frac{1000(d - d_0)}{mdd_0} \tag{4}$$

$$\phi_{K(S)} = \frac{M_2\beta_s}{d} + \frac{1000(\beta_s d_0 - \beta_{s,0} d)}{mdd_0} \tag{5}$$

where β_s and $\beta_{s,0}$ are the adiabatic compressibilities of the solution and water, respectively, calculated by using eq 3.

The results are listed in Table I and shown in Figures 4 and 5 as plots against ionic strength. Inspection of the figures shows once again that the $ZnBr_2$ solutions display characteristic peculiar behavior while the properties of the $CaBr_2$ and NaBr are rather typical.

Table I. Densities, Relative Sound Velocities, Apparent Molal Volumes, Apparent Molal Compressibilities, and Hydration Numbers of $ZnBr_2$, $CaBr_2$, and NaBr at 25 °C

m, mol·kg^{-1}	$10^3(d - d_0)$, g·cm^{-3}	$u - u_0$, m·s^{-1}	ϕ_V, cm^3·mol^{-1}	$-10^4\phi_K$, cm^3·mol^{-1}·bar^{-1}	n_{hydr}
			$ZnBr_2$		
0.2305	45.44	2.38	26.37	79.59	9.8
0.2501	49.28	2.44	26.36	78.92	9.7
0.3026	59.27	2.68	27.23	76.81	9.5
0.3176	62.23	2.70	27.09	76.48	9.4
0.3329	65.18	2.61	27.15	75.81	9.4
0.3468	67.71	2.41	27.60	74.70	9.2
0.3629	70.93	2.81	27.32	75.13	9.3
0.4200	81.52	2.15	28.32	71.96	8.9
0.4903	94.04	1.06	30.10	67.83	8.4
0.5624	106.93	−0.63	31.27	64.08	7.4
0.6401	120.76	−2.88	32.20	60.47	7.5
0.7126	133.96	−5.33	32.42	57.77	7.1
0.9521	176.30	−18.37	33.66	47.72	5.9
1.2501	227.27	−34.83	35.02	39.19	4.8
1.5014	267.64	−44.75	36.71	34.77	4.3
1.7487	307.10	−53.26	37.63	31.87	3.9
1.9987	345.84	−59.64	38.47	29.86	3.7
2.2496	382.57	−65.33	39.61	27.87	3.5
2.5187	422.67	−70.15	40.08	26.59	3.3
			$CaBr_2$		
0.4000	65.15	10.38	34.40	69.07	8.5
0.4249	68.98	11.13	34.80	68.56	8.5
0.5001	80.86	13.07	35.01	67.44	8.3
0.5998	96.09	15.78	35.90	65.63	8.1
0.8997	141.53	24.10	37.00	61.74	7.6
1.0515	163.27	28.15	38.07	59.41	7.3
1.3279	190.54	33.34	38.34	57.54	7.1
1.5012	229.32	40.42	38.08	55.42	6.9
1.6663	251.66	44.69	38.79	53.54	6.6
1.7239	261.10	46.27	38.15	53.52	6.6
2.0017	298.90	53.28	38.69	50.98	6.3
2.1025	313.29	55.88	38.51	50.36	6.1
2.3335	344.13	61.35	38.77	48.51	6.0
2.5952	378.68	67.64	38.93	46.68	5.8
			NaBr		
1.0000	85.07	29.92	25.25	35.17	4.4
1.5797	116.68	41.54	25.80	33.52	4.1
1.9972	144.25	52.28	26.70	31.70	3.9
2.4066	171.34	62.63	26.93	30.41	3.8
3.001	209.64	77.21	27.20	28.74	3.6
3.4833	239.99	88.82	27.33	27.54	3.4
3.9955	271.51	100.84	27.40	26.39	3.3
5.1927	342.50	127.77	27.44	24.08	3.0
8.3433	512.65	190.56	27.35	19.49	2.4

In our calculations we used the Pitzer equations in the forms reported recently by Anathaswamy and Atkinson (*15*). The equation for the apparent molal volume is

$$\phi_V = \phi_V{}^0 + |Z_M Z_X|(A_V/2b)\ln(1 + bI^{1/2}) + RT(\nu_M\nu_X/\nu)mB_{MX}{}^V + RT(\nu_M\nu_X)^{3/2}m^2c_{MX}{}^V \quad (6)$$

where

$$B_{MX}{}^V = 2\left(\frac{\partial\beta_{MX}{}^{(0)}}{\partial P}\right)_T + 2\left(\frac{\partial\beta_{MX}{}^{(1)}}{\partial P}\right)_T\frac{1}{\alpha^2 I}[(1 + \alpha I^{1/2} - \alpha^2 I/2)\exp(-\alpha I^{1/2})] \quad (7)$$

$$C_{MX}{}^V = \left(\frac{\partial C_{MX}{}^\phi}{\partial P}\right)_T - \frac{2}{3}\left(\frac{\partial B_{MX}{}^V}{\partial m}\right)_T \quad (8)$$

The equation for the apparent molal compressibility has the form

$$\phi_K = \phi_K{}^0 - |Z_M Z_X|(A_K/2b)\ln(1 + bI^{1/2}) - RT(\nu_M\nu_X/\nu)mB_{MX}{}^K - RT(\nu_M\nu_X)^{3/2}m^2C_{MX}{}^K \quad (9)$$

where $B_{MX}{}^K$ and $C_{MX}{}^K$ are the pressure derivatives of $B_{MX}{}^V$ and $C_{MX}{}^V$, respectively.

Therefore, the data were fitted to the Pitzer equations, holding $\alpha = 2.0$ and $b = 1.2$, as used by Pitzer, and $\phi_V{}^0$ or $\phi_K{}^0$ constant. The parameters are

$$\beta_V{}^{(0)} = \left(\frac{\partial\beta_{MX}{}^{(0)}}{\partial P}\right)_T,\quad \beta_V{}^{(1)} = \left(\frac{\partial\beta_{MX}{}^{(1)}}{\partial P}\right)_T,\quad C_{MX}{}^V$$

and their pressure derivatives $\beta_K{}^{(0)}$, $\beta_K{}^{(1)}$, and $C_{MX}{}^K$.

The calculations were performed using the corrected values of the slopes A_B and A_K, 1.874 and -3.778×10^{-4}, respectively, calculated by Ananthaswamy and Atkinson (*15*).

Tables II and III give the resulting Pitzer parameters for the $CaBr_2$ and NaBr solutions along with the corresponding limiting values calculated from the literature data. The limiting parameters for $ZnBr_2$ are also included. No attempt was made to fit the $ZnBr_2$ data with the Pitzer equations.

The Pitzer equations describe satisfactorily the variation of the apparent molal volume and adiabatic compressibility of the $CaBr_2$ and NaBr solutions up to ionic strength 8.0 M. The corresponding deviations are somewhat greater for the solutions of $CaBr_2$. The same difference was observed previously by Kumar and Atkinson for the $CaCl_2$ and NaCl solutions (*2*). They were convinced that this was due to the nature of the Pitzer equation. The hydration sphere of the Ca^{2+} cation is changing in the concentration range above 1.0 M (*16*) and there is no simple way to accommodate this phenomena in the theory.

The limiting values of $\phi_V{}^0$ and $\phi_K{}^0$ are in reasonable agreement with those calculated from the low concentration literature data for $CaCl_2$ (*2*) and NaCl (*2*), and NaBr (*14*), $ZnCl_2$ (*17*), and $Zn(NO_3)_2$ (*18*). Complete agreement should not be expected since the low-concentration form of the Pitzer equations is not optimal for infinite dilution extrapolation. The $\phi_V{}^0$'s and $\phi_K{}^0$'s we present are optimized for the best representation of the data over the whole concentration range.

The peculiar nature of the $ZnBr_2$ solutions is made abundantly clear in Figures 4 and 5. Here we have used $\phi_V{}^0$ and $\phi_K{}^0$

Table II. Pitzer Coefficients for Apparent Molal Volumes of NaBr and $CaBr_2$ at 25 °C

salt	$\phi_V{}^0$, cm^3·mol^{-1}	$10^5\beta_V{}^{(0)}$	$10^5\beta_V{}^{(1)}$	$10^6C_{MX}{}^V$	σ, cm^3·mol^{-1}
NaBr	23.50	1.5 (±0.3)	1.3 (±2.2)	−2.8 (±0.6)	0.20
$CaBr_2$	32.37	4.3 (±0.8)	−39.9 (±5.5)	−17.7 (±3.6)	0.36
$ZnBr_2$	25.00				

Table III. Pitzer Coefficients for Apparent Molal Compressibilities of NaBr and $CaBr_2$ at 26 °C

salt	$-10^4\phi_K{}^0$, cm^3·mol^{-1}·bar^{-1}	$10^9\beta_K{}^{(0)}$	$10^9\beta_K{}^{(1)}$	$10^{10}C_{MX}{}^K$	$10^4\sigma$, cm^3·mol^{-1}·bar^{-1}
NaBr	41.8	−6.8 (±0.3)	−5.7 (±2.1)	6.5 (±0.5)	0.17
$CaBr_2$	77.83	−12.4 (±0.6)	47.3 (±4.1)	23.3 (±2.6)	0.27
$ZnBr_2$	90.3				

values obtained from the additivity principle using ϕ_V^0 data from unassociated salts. ϕ_V for $ZnBr_2$ will have to do some very peculiar gyrations to approach the expected ϕ_V^0.

It is now useful to at least qualitatively describe the $ZnBr_2$ volumetric data in terms of the known chemistry of the system. The apparent molal volume behavior of "normal" electrolytes can be described by a term, ϕ_V^0, characteristic of the effect of the isolated ions on the water plus terms describing both the long-range and short-range electrostatic interactions. Since the number of waters per ion decreases with increasing m, the effects tend to saturate at high m. Similarly, when we compress a "normal" electrolyte solution, we are compressing the rather open water structure not the ions. In fact, waters very close to ions are already under very high fields and have a lower compressibility than bulk water. This effect becomes larger with smaller ions of higher charge.

We can write a simple complexation reaction as

$$Zn(H_2O)_6^{2+} + Br^-(aq) \rightarrow [ZnBr(H_2O)_3]^{1+} + nH_2O(aq)$$

Our vagueness concerning $Br^-(aq)$ hydration compared to $Zn^{2+}(aq)$ is based on lack of experimental data. But regardless of detail, such complexation reactions clearly release "free" water and have a positive ΔV. This appears as an increase in ϕ_V on complex ion formation. So the only real peculiarities in our $ZnBr_2$ ϕ_V data are the rather abrupt changes in the slope of the ϕ_V vs. $I^{1/2}$ curve. These imply that we do not have a gradual, statistically controlled progression from ZnX^+ to ZnX_4^{2-}. Rather, it implies that one or two of the complexes are thermodynamically favored. The ϕ_K curve represents a logical extension of this same idea; that is, the released free waters are substantially more compressible than those next to an ion. Furthermore, all of the usually postulated complex ions in this system $ZnBr^+$, $ZnBr_2^0$, $ZnBr_3^{1-}$, and $ZnBr_4^{2-}$ would exert a smaller compressive field on the surrounding waters than the parent Zn^{2+}. As Nicholas and Reich have implied these effects could be augmented or diminished by vaguer "structure-making" and "structure-breaking" effects of the ion mixture.

A dramatic if approximate way of illustrating the above is the calculation of the apparent hydration numbers by the Passynski equation (*18*)

$$n = \frac{1000}{mM_1}\left(1 - \frac{u_0^2 d_0^2}{u^2 d^2}\,\frac{1000 + mM_2}{1000}\right)$$

where n is the apparent hydration number of the salt, M_1 is the formula weight of solvent, and M_2 is the formula weight of solute. This equation assumes that the waters of hydration are incompressible and that no ion–ion forces prevail! The results are given in Table I and illustrated in Figure 6. This shows that the apparent hydration number of the $ZnBr_2(aq)$ ions drops dramatically as complexation occurs. At high concentrations it is closer to the value for NaBr than for $CaBr_2$. The numbers reported for NaBr are very similar to those reported by Bockris and Saluja (*20*).

Conclusions

The apparent molal volumes and compressibilities of aqueous NaBr and $CaBr_2$ solutions are described very adequately by the Pitzer formalism. However, the thermodynamic properties of aqueous $ZnBr_2$ clearly place it outside the category of simple electrolytes for which the Pitzer formalism was designed. Inflection points in plots of a given property vs. concentration are caused by Zn^{2+}–Br^- complex formation. Furthermore, the presence of such inflections strongly imply that the relationship between successive stability constants is not governed by simple statistical factors. Additional evidence for this was recently presented by Goggin and his co-workers (*21*) using X-ray and Raman techniques. In 2.5 M $ZnBr_2$, for example, they found $[Zn^{2+}] = 1.42$, $[ZnBr^+] \simeq 0$, $[ZnBr_2] = 0.25$, $[ZnBr_3^-] = 0.48$, and $[ZnBr_4^{2-}] = 0.36$ M. This implies an abnormal stability for the higher complexes compared to the lower. The Pitzer formalism can, in principle, be applied to such cases. But the number of interaction coefficients needed increases dramatically and there is a severe problem of redundancy between the Pitzer coefficients and the thermodynamic stability constants. These problems would be exacerbated in mixtures of $ZnBr_2$ with other simpler halide salts.

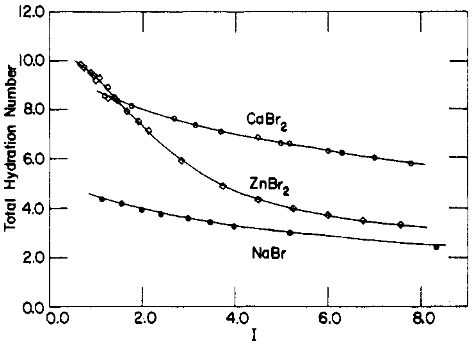

Figure 6. Plot of the total hydration number against the ionic strength at 25 °C.

Registry No. NaBr, 7647-15-6; $CaBr_2$, 7789-41-5; $ZnBr_2$, 7699-45-8.

Literature Cited

(1) Pitzer, K. S. *Activity Coefficients in Electrolyte Solutions* Pytkowicz, R. M., Ed.; CRC Press: Boca Raton, FL, 1979; Vol. 1, Chapter 7.
(2) Kumar, A.; Atkinson, G.; Howell, R. D. *J. Solution Chem.* **1982**, *11*, 857–870.
(3) Kumar, A.; Atkinson, G. *J. Phys. Chem.* **1983**, *87*, 5504–5507.
(4) Kalman, E.; Suke, I.; Palinkas, G.; Johansson, G.; Kabisch, G.; Maida, M.; Ohtaki, H. *Z. Naturforsch.* **1983**, *38a*, 225–230.
(5) Tamura, K. *J. Phys. Chem.* **1977**, *81*, 820–826.
(6) Robinson, R. A.; Harned, H. S. *Chem. Rev.* **1941**, *28*, 419–476.
(7) Goldberg, R. N.; Nuttal, R. L. *J. Phys. Chem. Ref. Data* **1978**, *7*, 263–310.
(8) Goldberg, R. N.; Nuttal, R. L. *J. Phys. Chem. Ref. Data* **1981**, *10*, 1–55.
(9) Nicholas, M.; Reich, R. *Nouv. J. Chim.* **1982**, *6*, 467–476.
(10) Flaschka, H. A. *EDTA Titrations*; Pergamon: New York, 1959.
(11) Vogel, A. I. *A Textbook of Quantitative Inorganic Analysis*; Longmans-Green: London, 1951.
(12) Chen, C.-T.; Chen, L.-S.; Millero, F. J. *J. Acoust. Soc. Am.* **1978**, *63*, 1795–1800.
(13) Perron, G.; Roux, A.; Desnoyers, J. E. *Can. J. Chem.* **1981**, *59*, 3049–3054.
(14) Millero, F. J.; Ward, G. K.; Chetirkin, P. *J. Acoust. Soc. Am.* **1977**, *51*, 1492–1498.
(15) Ananthaswamy, J.; Atkinson, G. *J. Chem. Eng. Data* **1984**, *29*, 81–87.
(16) Hewish, N. A.; Neilson, G. W.; Enderbg, J. E. *Nature (London)* **1982**, *297*, 138–139.
(17) Surdo, A. Lo.; Millero, F. J. *J. Phys. Chem.* **1980**, *84*, 710–715.
(18) Spitzer, J. J.; Singh, P. P.; Olofsson, I. V.; Hepler, L. G. *J. Solution Chem.* **1978**, *7*, 623–629.
(19) Passynski, A. *Acta Physicochim. URSS* **1938**, *8*, 385–418.
(20) Bockris, J. O'M; Saluja, P. P. S. *J. Phys. Chem.* **1972**, *76*, 2140–2151.
(21) Goggin, P. L.; Johansson, G.; Maida, M.; Wakita, H. *Acta Chem. Scand., Ser. A* **1984**, *A38*, 825–639.

Received for review October 21, 1985. Accepted January 13, 1986. We acknowledge the support of this work by the National Science Foundation under Grant CPE 8017441 and by the Amoco Production Co. of Tulsa, OK.